

RESEARCH ARTICLE

Sensory Processing

Individual magnitudes of neural variability quenching are associated with motion perception abilities

Edan Daniel^{1,2,3} and Ilan Dinstein^{1,2,3}¹Department of Brain and Cognitive Science, Ben Gurion University of the Negev, Beer-Sheva, Israel; ²Department of Psychology, Ben Gurion University of the Negev, Beer-Sheva, Israel; and ³Zlotowski Center for Neuroscience, Ben Gurion University of the Negev, Beer-Sheva, Israel

Abstract

Remarkable trial-by-trial variability is apparent in cortical responses to repeating stimulus presentations. This neural variability across trials is relatively high before stimulus presentation and then reduced (i.e., quenched) ~ 0.2 s after stimulus presentation. Individual subjects exhibit different magnitudes of variability quenching, and previous work from our lab has revealed that individuals with larger variability quenching exhibit lower (i.e., better) perceptual thresholds in a contrast discrimination task. Here, we examined whether similar findings were also apparent in a motion detection task, which is processed by distinct neural populations in the visual system. We recorded EEG data from 35 adult subjects as they detected the direction of coherent motion in random dot kinematograms. The results demonstrated that individual magnitudes of variability quenching were significantly correlated with coherent motion thresholds, particularly when presenting stimuli with low dot densities, where coherent motion was more difficult to detect. These findings provide consistent support for the hypothesis that larger magnitudes of neural variability quenching are associated with better perceptual abilities in multiple visual domain tasks.

NEW & NOTEWORTHY The current study demonstrates that better visual perception abilities in a motion discrimination task are associated with larger quenching of neural variability. In line with previous studies and signal detection theory principles, these findings support the hypothesis that cortical sensory neurons increase reproducibility to enhance detection and discrimination of sensory stimuli.

individual differences; motion perception; neural variability; trial-by-trial variability quenching; variability quenching

INTRODUCTION

Although our perception of the world around us seems stable, remarkable trial-by-trial variability is apparent in cortical neural activity even across trials containing an identical stimulus. A variety of studies have demonstrated that neural variability across trials is large before the presentation of a stimulus and then reduced (quenched) ~ 200 ms after stimulus presentation. This stimulus-induced quenching of neural variability is apparent in intracellular and extracellular recordings of individual neurons (1, 2), as well as in cortical population activity recorded by electroencephalography (EEG), magnetoencephalography (MEG), and functional magnetic resonance imaging (fMRI) (3–10). This variability quenching is

tightly coupled with a reduction in neural oscillations in the alpha-beta frequency band (11), thereby creating more reproducible cortical responses across trials (10).

The magnitude of variability quenching following stimulus presentation differs across individuals in a consistent manner such that some subjects exhibit larger variability quenching than others (4). Previous work from our laboratory has demonstrated that individuals with larger magnitudes of variability quenching exhibit lower (i.e., better) perceptual thresholds when performing a contrast discrimination task (5). This finding is in line with principles of signal detection theory whereby reducing variability increases the ability to detect a signal (12). If the magnitude of variability quenching indeed has a beneficial impact on perceptual performance, it should be evident in other perceptual tasks.

With this in mind, we decided to examine the relationship between variability quenching and the perception of coherent motion using random dot kinematograms.

Contrast discrimination and coherent motion detection are two tasks that rely on distinct neural populations within the visual system. Perception of visual motion relies on direction-selective neurons that are located primarily in primary visual cortex (V1) and the middle temporal (MT/V5) area (13). Neurons in area MT have larger receptive fields than neurons in V1, and this distinction makes MT neurons specifically important for the perception of coherent motion when using random dot kinematograms. Kinematograms contain moving dots positioned in multiple locations of the visual field, and detection of the direction of their coherent motion requires integration across relatively large spatial fields (14, 15). Furthermore, microstimulating neurons in area MT are sufficient for altering the perception of coherent motion in monkeys (16). These studies and others have demonstrated that motion perception requires the integration of V1 inputs into area MT (17).

Unlike coherent motion perception, contrast detection and discrimination do not require the integration of V1 inputs into a higher area of the visual system. Rather, contrast sensitivity is captured by the responses of V1 neurons such that increasing stimulus contrast generates an increase in neural firing rates (18). Furthermore, contrast discrimination does not rely on the responses of MT/V5 neurons, which are not modulated by contrast levels (19, 20). Although MT lesions dramatically impair the perception of coherent motion, they do not affect contrast discrimination thresholds (21).

To assess the relationship between neural variability magnitudes and coherent motion perception, we recorded EEG data from 35 adult subjects as they performed a motion detection task using random dot kinematograms. The stimuli contained varying degrees of coherent motion, which enabled us to estimate a psychometric function and threshold for coherent motion detection in individual subjects (21–24). To manipulate task difficulty, participants performed the task at three different dot densities. Since coherent motion is easier to detect in kinematograms with higher dot densities (25), this manipulation enabled us to further examine whether individual magnitudes of variability quenching were associated with the subjects' perceptual thresholds at varying degrees of task difficulty.

MATERIALS AND METHODS

Subjects

Thirty-five subjects (51% females, 24.8 ± 2 yr old, range: 21–30 yr old) successfully completed the study and were included in all analyses. All subjects were right-handed, had normal or corrected-to-normal vision, and no known history of learning disabilities or attention disorders. The experiment was conducted in accordance with the Declaration of Helsinki and approved by the ethics committee of Ben Gurion University of the Negev. Each subject gave written informed consent and received either payment (28\$US) or research credit as part of their undergraduate program. An additional 20 subjects participated in the study but were excluded from the analysis

due to insufficient number of trials after cleaning (13 subjects with <250 trials), unreasonable threshold estimation (three subjects with motion coherence thresholds > 0.5), flawed recording (two subjects), inability to learn the task (one subject), and strabismus (one subject).

Experimental Design

Subjects were seated in a dark soundproof room, with their head positioned on a chin rest, 80 cm from a CRT monitor (refresh rate: 60 Hz, resolution: 1280×1024 pixels). Stimuli were generated using MATLAB (MathWorks Inc.) and Psychtoolbox (26–28). The experiment consisted of a single 2-h recording session and included two parts: a coherent motion detection task (Fig. 1) and passive observation of a flickering checkerboard. Only data from the first task are included in the current study.

Coherent Motion Task

We used a random dot kinematogram (21, 24), composed of a circular area with white dots (diameter = 12° , dot diameter = 0.7°) that were presented on a black background. Dots moved at a speed of $5^\circ/\text{s}$ in random directions, with a subset of the dots moving coherently to the left or right. Each dot had a limited lifetime of 0.25 s after which it disappeared and reappeared in a new random location. We presented the stimulus at three different dot densities (0.6, 1.8, or $5.4 \text{ dots}/\text{deg}^2$, corresponding to 68, 204, or 611 dots). Dot density was consistent within each block (i.e., set of 100 trials), and subjects completed three blocks (300 trials) with each dot density. A white fixation cross was presented at the center of the screen throughout the experiment.

Each trial consisted of a stimulus (0.67 s), waiting period (0.6 s), response cue, and a random intertrial interval (ITI; 0.9/1.1/1.2 s). Participants were instructed to focus their gaze on the fixation cross throughout the experiment and wait for the fixation cross to change color from white to gray (i.e., response cue) before reporting the direction of coherent motion by pressing the corresponding arrow key on the keyboard.

The coherence level presented on individual trials was selected using the Psi method (29, 30), a Bayesian adaptive method for optimal estimation of the threshold and slope of the psychometric function. This technique uses the data from completed trials to update a posterior probability distribution used to select the coherence level of the next trial (31, 32). This enables selection of coherence levels that maximize the expected information gain (minimize entropy) for estimating the threshold and slope (33).

Before starting the experiment, subjects practiced the task with 80% coherence and a random dot density. They received feedback on each trial (fixation cross turned green for correct and red for incorrect). The practice session ended when the subject performed 10 correct responses in a row.

EEG and Eye-Tracking Data Acquisition

EEG data were recorded using a 64-channel Bio-Semi system (Biosemi, Inc) at 1024 Hz, referenced to the mastoid electrodes. Electrooculography was recorded using two electrodes placed on the outer canthi of the left and right eyes, and one electrode placed below the right eye. The position of the right

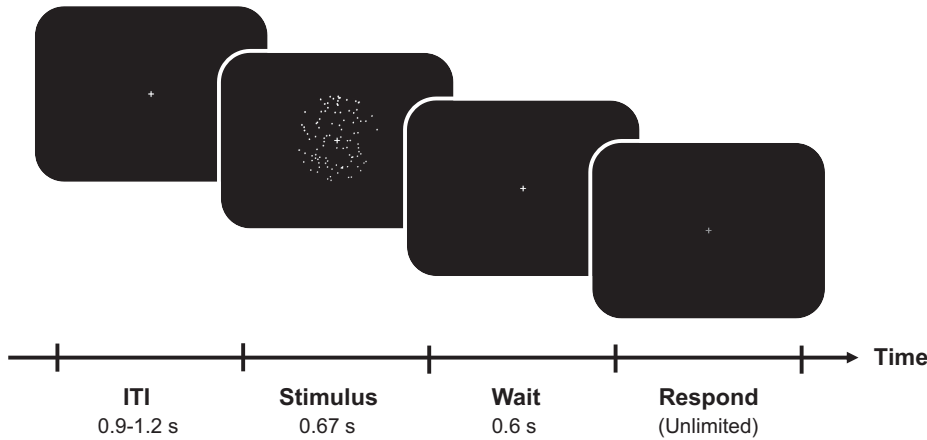


Figure 1. Design of the coherent motion task. The stimulus consisted of a circular area with white dots. A proportion of the dots moved coherently to the right or left and the remaining dots moved in random directions. Subjects were requested to wait for the fixation cross to turn gray before reporting the direction of coherent motion by pressing one of two keys. Each trial was followed by a jittered intertrial interval (ITI).

eye was simultaneously recorded with an eye tracker at 1000 Hz (EyeLink 1000; SR Research Ltd).

EEG Preprocessing

EEG data were analyzed in MATLAB (MathWorks, Inc.) using the EEG toolbox (34) and EYE-EEG toolbox (35). Continuous EEG data were down-sampled to 512 Hz and filtered using 1 Hz high-pass and 40 Hz low-pass Hamming windowed finite impulse response (FIR) filters. Continuous data were cut into epochs, from 0.5 s before to 1.8 s after stimulus onset. Epochs (i.e., trials) with absolute signal amplitude $>70 \mu\text{V}$ in any of the frontal electrodes (Fp1, Fp2, AF3, AF4, AF7, AF8), or power >25 db in the 20–40 Hz frequency range, were automatically identified and removed—these criteria typically remove trials with eye blinks and teeth clenching artifacts. Additional trials with eye blinks located between -0.25 s to $+1$ s of stimulus onset were identified using the eye tracker and removed. In addition, trials containing horizontal or vertical eye movements that were larger than 15% of the screen size (3.2° vertical, 4.0° horizontal) were removed. Subjects with less than 250 clean trials were excluded from the analyses. The remaining 35 subjects had an average of 609 (± 184) clean trials per subject. Unless otherwise stated, we averaged data over six occipital/parietal electrodes (P6, P8, PO8, P5, P7, and PO7) that best captured the responses to the stimuli, as performed previously in our contrast discrimination study (5) and other neural variability studies using visual stimuli (3, 4, 11).

Neural Variability Analyses

Trial-by-trial variability was computed for each time point in every electrode. Importantly, this step was performed on the raw data of individual trials, without normalizing the EEG signal in any way (i.e., without baseline correction, which is often performed in ERP analyses and is not relevant here). Absolute trial-by-trial variability in the prestimulus (Var_{pre}) and poststimulus (Var_{post}) periods were computed by averaging the trial-by-trial variability across the relevant time-points (-0.25 s to stimulus onset and 0.3 to 0.7 s after stimulus onset, respectively). Relative change in trial-by-trial variability (i.e., variability quenching) was then estimated by dividing the variability in the poststimulus period by the

variability in the prestimulus period and adjusting to percent change units, as follows:

$$\text{Neural Variability Quenching} = \left(\frac{Var_{post}}{Var_{pre}} - 1 \right) \cdot 100$$

Psychometric Function Estimation

The coherent motion detection threshold and psychometric function slope were estimated for each subject using a maximum likelihood method as implemented in the Palamedes Toolbox (33). Data aggregated for each subject from all blocks were fitted as follows:

$$\psi(x; \alpha, \beta, \gamma, \lambda) = \gamma + (1 - \gamma - \lambda) * F(x; \alpha, \beta)$$

where ψ represents the performance level (i.e., proportion correct), x refers to the stimulus coherence level and γ and $1 - \lambda$ correspond to the lower and upper asymptote of the psychometric function, respectively. The lower asymptote corresponded to the guess rate (γ) that was set to 0.5 (i.e., chance level given the two-alternative forced choice task), and the upper asymptote was assumed to be governed by an attention-lapse rate (λ) of 0.02 (i.e., upper asymptote was assumed to be 0.98 performance level). The sigmoidal function used was a Gumbel (logarithmic Weibull) function, defined as:

$$F(x; \alpha, \beta) = 1 - e^{-10^{\beta(x-\alpha)}}$$

where x refers to the stimulus coherence level, α to the perceptual threshold, and β the slope of the psychometric function. The coherent motion threshold (set to 74% correct) and psychometric function slope were extracted for each subject separately while including coherence levels that were sampled at least three times.

Goodness-of-Fit

To quantify the quality of fit between the estimated psychometric function (\hat{y}) and the observed data (y), we calculated the root mean square error (RMSE) for each individual subject, as defined by:

$$RMSE = \sqrt{\frac{\sum_{i=1}^N (\hat{y}_i - y_i)^2}{N}}$$

where N is the number of coherence levels. The RMSE of all subjects fell within ± 2.5 SD of the mean RMSE across

subjects, demonstrating a reasonable fit for all subjects with no extreme outliers.

Electrode Offset Variability

To assess the quality of individual EEG recordings and ensure that potential individual differences in data quality did not affect our findings, we examined electrode offset in individual subjects. Electrode offset is a measure that quantifies the amplitude of slow changes in voltage potential over time, which is indicative of the quality of the EEG recording when using active electrode systems where impedance is not measured (36). We computed the trial-by-trial variability of electrode offsets in each of the six electrodes used in the main analyses and then averaged across electrodes in each subject. We then examined whether individual differences in the variability of electrode offset could explain individual differences in neural variability quenching by computing the Pearson correlation across the two measures.

Eye-Gaze Variability

Even small eye movements are known to generate considerable changes in voltage potential when recording EEG (37). To ensure that individual differences in eye movements did not affect our results, we calculated the Euclidian distance in pixels between the gaze position as reported by the eye tracker and the fixation cross at each time-point (gaze position was sampled at 1,000 Hz). We then computed the variability of this measure in the poststimulus time window (i.e., 0.3–0.7 s after stimulus onset) of each trial and averaged across trials per subject. This measure of eye-gaze variability, in units of squared pixels, was computed for each subject and used to quantify eye movements (i.e., larger variability = more eye movements). We then computed the Pearson correlation between this measure and individual magnitudes of EEG variability quenching to test whether the measures were related.

Statistical Tests

Relationships between pairs of measures such as absolute trial-by-trial variability, neural variability quenching, motion coherence threshold, electrode offset, and goodness-of-fit were estimated using Pearson's correlations. The significance of these correlations was estimated using a permutation/randomization test. This procedure included shuffling the labels of vectors before calculating the correlation between them (i.e., shuffling the data of individual subjects). This procedure was performed 10,000 times, with each iteration yielding a correlation coefficient that was based on a different randomization. The resulting correlation coefficients represented a null distribution of random results given the distribution of the initial measures across the subjects in the study. For the true correlation coefficient to be considered significant, it had to be higher than the 95th percentile or lower than the 5th percentile of this null distribution.

To assess the consistency of findings across our current and previous studies regarding the relationship between perceptual thresholds and variability quenching, we computed the Bayes factor, using JASP (38). The Bayes factor quantifies the evidence for the null hypothesis compared with an alternative hypothesis given a prior. Here, we tested whether

there was evidence for a significant correlation between motion coherence thresholds and variability quenching in our data, given the correlation between coherence discrimination thresholds and variability quenching that was reported by Arazi et al. (5) (i.e., the prior). Conventionally, a Bayes factor that is >3 offers strong support for the alternative hypothesis, and one lower than $1/3$ provides strong support for the null hypothesis (39). Comparisons of individual measures such as coherent motion thresholds across different dot densities were performed using pairwise *t* tests.

Data Availability

Raw data will be made available upon reasonable request from the authors.

RESULTS

Subjects exhibited typical event-related potential (ERP) responses to the presentation of the random dot kinematograms (Fig. 2A). On average, trial-by-trial variability was reduced/quenched by 31%, relative to prestimulus variability (Fig. 2B). Variability quenching reached full strength ~ 200 ms after stimulus presentation and was strongest in electrodes covering occipital and parietal cortices (Fig. 2D). P100 responses were also strongest at occipital-parietal sensors (Fig. 2C).

Variability Quenching and Dot Density

Trial-by-trial variability was quenched from ~ 0.2 s to ~ 1 s after stimulus presentation (Fig. 2B). The magnitude of variability quenching was similar across different dot densities (Fig. 3). Furthermore, individual magnitudes of variability quenching were highly correlated across dot densities (Fig. 3B), demonstrating that the magnitude of variability quenching was a stable trait of individual subjects, as also reported in previous studies (4, 5). Strong and significant correlations were apparent between individual magnitudes of variability quenching at different dot densities (low vs. medium: $r = 0.94$, $P < 0.001$; low vs. high: $r = 0.90$, $P < 0.001$; and medium vs. high: $r = 0.90$, $P < 0.001$). Note that the number of moving elements in the high dot density stimulus (611 moving dots) was an order of magnitude larger than the number of elements in the low density stimulus (68 moving dots). This difference in the stimulus density had a significant effect on perceptual thresholds (see next section) but not on the magnitude of variability quenching.

Motion Coherence Thresholds

We fit a sigmoidal psychometric function to the behavioral data of each subject (Fig. 4A) and extracted the function's slope and threshold (i.e., coherence percentage necessary to achieve 74% discrimination accuracy). This procedure was performed separately for stimuli containing low, medium, and high dot densities. Subjects with unreasonable thresholds ($>50\%$) in each dot density were excluded from this analysis (i.e., $N = 34$, 32, and 31 in the low, medium, and high densities, respectively). We noted significant differences in motion coherence thresholds across stimuli with different dot densities (Fig. 4B). Specifically, higher (i.e., poorer) thresholds were apparent when presenting subjects with

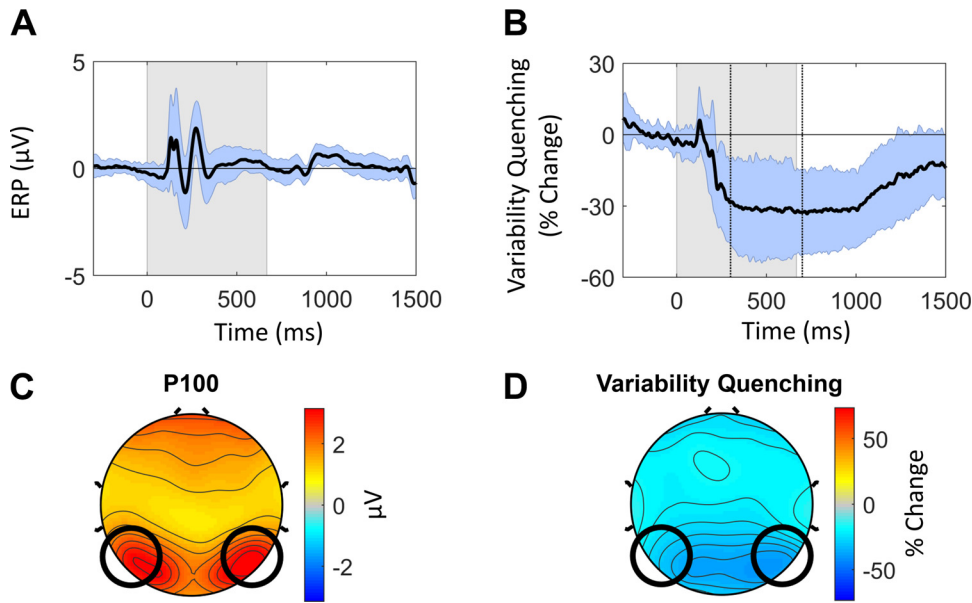


Figure 2. Cortical responses to the coherent motion stimulus. **A:** mean ERP across subjects (black line, $N = 35$) and standard deviation across subjects (shaded blue). Gray shaded area: time of stimulus presentation. **B:** trial-by-trial variability in units of percent change relative to the prestimulus period (-0.25 s to stimulus onset). Mean across subjects (black line) and standard deviation across subjects (shaded blue). Gray shaded area: time of stimulus presentation. Dashed black vertical lines: limits of time window used to calculate individual magnitudes of variability quenching. **C:** topographic map of early visual responses at P100, demonstrating that the largest visual responses (darker red) were apparent in occipital-parietal electrodes. **D:** topographic map of variability quenching demonstrating that larger quenching (darker blue) was also apparent in the same occipital-parietal electrodes. ERP, event-related potential.

stimuli containing low dot densities in comparison with medium ($t = 4.31, P < 0.001$) or high ($t = 4.87, P < 0.001$) dot densities. Thresholds did not differ significantly between the medium and high dot densities ($t = 1.05, P = 0.302$).

Variability Quenching Magnitudes and Coherent Motion Thresholds

Coherent motion thresholds that were computed across all trials (regardless of dot density) were positively correlated with individual magnitudes of neural variability quenching ($r = 0.38, P = 0.019$; Fig. 5A) such that subjects with lower thresholds (i.e., better perceptual ability) had larger magnitudes of variability quenching (i.e., larger decreases in variability). We also note that there was a negative correlation between the slope of the psychometric function and the magnitude of neural variability quenching, yet this correlation was not statistically significant ($r = -0.12, P = 0.29$; Fig. 5B). Note that the significance of these correlations was tested with a randomization/permutation test.

We also examined the correlations between individual magnitudes of variability quenching and coherent motion

thresholds at each of the three stimulus dot densities separately (Fig. 5, C–E). This analysis revealed that the relationship was significant only when analyzing trials with low dot density ($r = 0.37, P = 0.03$), such that the correlations became sequentially weaker when analyzing trials with medium ($r = 0.22, P = 0.13$) and high ($r = 0.13, P = 0.19$) dot densities.

Consistency across Studies

In a previous study, we found that individual magnitudes of variability quenching were significantly correlated with contrast discrimination thresholds (5). To determine the robustness of this relationship, which appeared in both the previous and current studies using distinct designs and tasks, we computed a Bayes factor. This analysis examines the strength of evidence for accepting the hypothesis whereby there is a significant correlation in the current study, given the evidence found in the previous study (i.e., the prior). Using the correlation value reported in the contrast discrimination study as the prior, the Bayes factor revealed that there was strong evidence for the existence of a consistent relationship between individual variability quenching

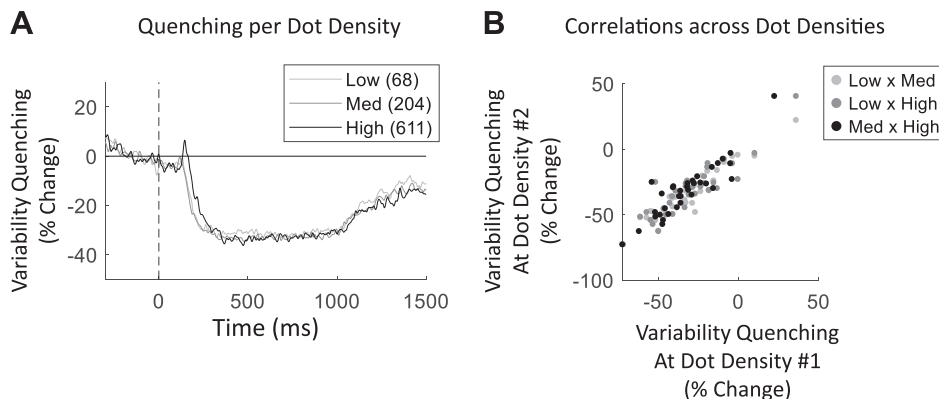
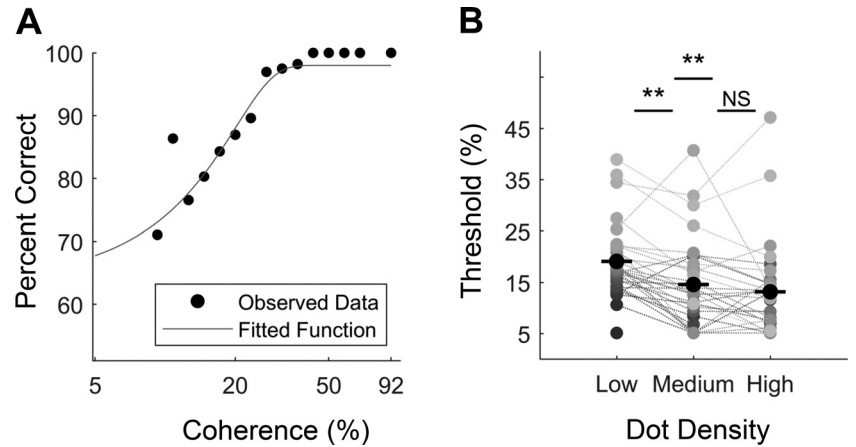


Figure 3. Trial-by-trial variability quenching is a stable individual trait, consistent across dot densities. **A:** trial-by-trial variability in units of percent change relative to the prestimulus period (-0.25 s to stimulus onset) in trials with low (68 dots), medium (204 dots), and high (611 dots) dot densities. **B:** scatter plot demonstrating the relationship between individual magnitudes of variability quenching across pairs of dot densities (light gray = low vs. medium; gray = low vs. high; dark gray = medium vs. high dot density). Each point represents a single subject ($N = 35$).

Figure 4. Motion coherence thresholds. *A*: psychometric function of *subject 2*. Each point represents the percent of correct answers (y) at a given coherence level (x). Gray line represents the maximum likelihood Gumbel (logarithmic Weibull) function that was fit to the presented data points. *B*: perceptual thresholds for each dot density. Each point represents the threshold of a specific subject. Dashed lines connect the threshold values of a single subject across the three dot densities. NS, not significant $**P < 0.001$.



and perceptual thresholds in the current study (Bayes factor = 6.65).

Absolute Variability Magnitudes and Coherent Motion Thresholds

Previous work from our laboratory has demonstrated that variability quenching measures explain perceptual abilities better than absolute neural variability measures (4, 5). To

reexamine this issue in the current study, we estimated absolute trial-by-trial variability in the prestimulus and poststimulus time periods (see METHODS). We then tested whether individual magnitudes of absolute variability were correlated with individual coherent motion thresholds. We found that both individual magnitudes of prestimulus variability ($r = -0.19, P = 0.28$) and poststimulus variability ($r = -0.13, P = 0.46$) were not significantly correlated with coherent motion thresholds.

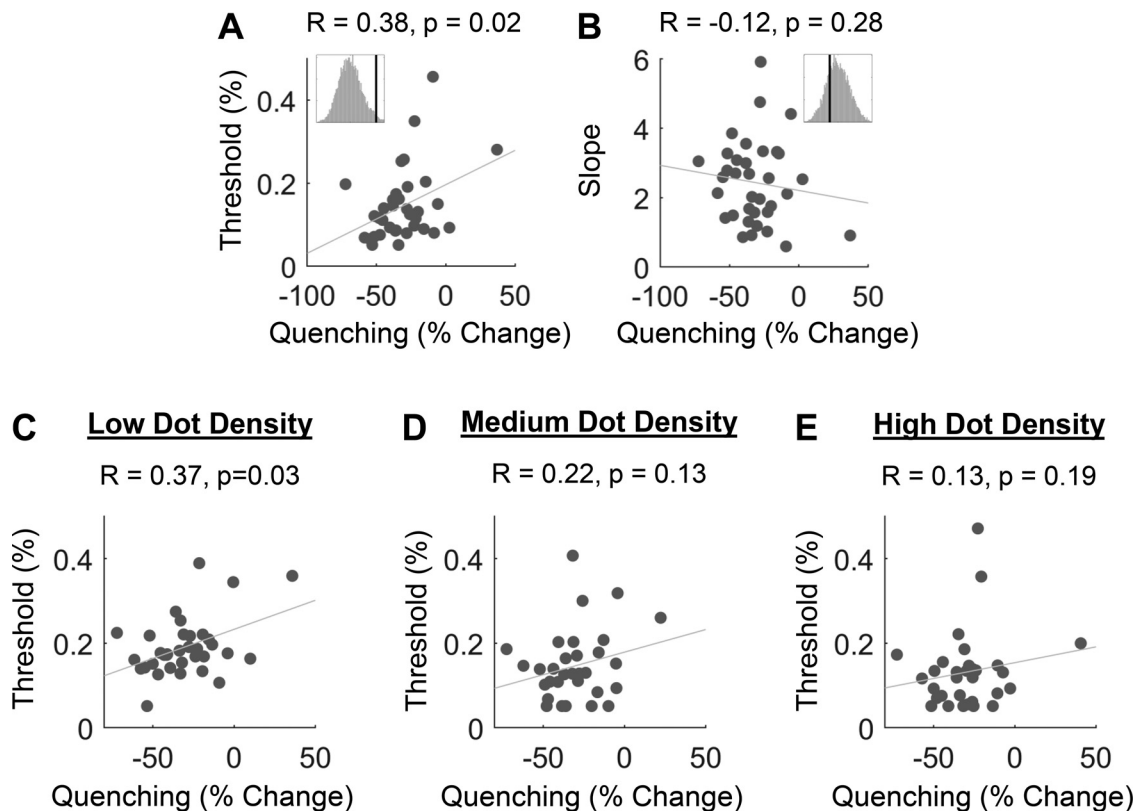


Figure 5. Variability quenching magnitudes and coherent motion perception. Scatter plots demonstrate the relationship between individual magnitudes of variability quenching and coherent motion thresholds (*A*) ($N = 35$) or the slope of the psychometric function (*B*). *Insets* demonstrate the randomization statistical test by presenting the null distribution of correlation coefficients when randomly shuffling subject identities 10,000 times. The actual correlation value is represented by the vertical black line. Separating the analysis according to dot densities revealed that individual magnitudes of variability quenching were specifically correlated with motion coherence thresholds that were based on trials with low dot densities (*C*) and more weakly correlated with motion coherence thresholds that were based on medium (*D*) and high (*E*) dot densities. Each point represents a single subject. Gray: least-square line.

Control Analyses

To ensure that our results were not generated by alternative nonneural sources of EEG variability, we performed several control analyses. First, we examined differences in the quality of the EEG recordings across individual subjects. When recording EEG with active electrode systems like Biosemi, the quality of the recording is often measured by low-frequency changes that are apparent in electrode offsets (see METHODS). Unstable recordings are characterized by changes in electrode offsets over time and across trials. Therefore, we computed the variability of electrode offsets across trials in individual subjects and computed their correlation with individual magnitudes of variability quenching. The two measures were not significantly correlated ($r = -0.26$, $P = 0.14$), suggesting that individual magnitudes of trial-by-trial variability were not generated by differences in the stability of individual recordings.

In another analysis, we examined the amount of eye movements performed by individual subjects, given that eye movements are expected to generate EEG artifacts leading to larger variability (37). We computed the gaze position variability as a measure of the amount of eye movements performed by each subject (see METHODS). We found that this measure was not correlated with individual magnitudes of variability quenching ($r = 0.11$, $P = 0.53$), demonstrating that the reported differences in neural variability quenching were not generated by individual differences in eye movements.

Furthermore, the number of rejected trials was not correlated with individual magnitudes of neural variability quenching ($r = -0.02$, $P = 0.91$), demonstrating that the amount of data available for individual subjects did not have an impact on the estimated trial-by-trial variability. The number of rejected trials was also not significantly correlated with individual perceptual thresholds ($r = -0.02$, $P = 0.88$), demonstrating that the amount of data available for individual subjects did not create a bias in their threshold estimations.

Finally, we performed a partial correlation analysis where we tested the relationship between the individual magnitudes of variability quenching and perceptual thresholds while controlling for all alternative variables described above. The partial correlation remained almost as strong as in the original analysis (Fig. 5A), and borderline significant ($r = 0.34$, $P = 0.058$), demonstrating that the correlation between trial-by-trial variability quenching and perceptual thresholds was barely affected by differences in the quality of EEG recording, eye movements, or number of rejected trials.

DISCUSSION

Our results demonstrate that individual subjects exhibit distinct magnitudes of variability quenching, which are significantly, albeit weakly, correlated with their coherent motion thresholds. Subjects with stronger variability quenching tended to have lower (better) perceptual thresholds in the motion detection task. This relationship was specifically evident when using stimuli with low dot densities (Fig. 5) where motion coherence was more difficult to identify (Fig. 4). This suggests that the magnitude of variability quenching may be particularly important for detecting ambiguous stimuli.

These findings suggest that a consistent association is apparent between individual magnitudes of variability quenching and individual perceptual abilities in the visual domain. The current study demonstrated this association in a motion discrimination task, whereas a previous study from our laboratory reported similar associations in a contrast discrimination task (5). Indeed, performing a Bayes factor analysis revealed that there was strong evidence across studies for accepting the significance of this relationship. Hence, converging evidence from two independent studies with different designs and tasks confirms that individual magnitudes of variability quenching are related to perceptual performance.

When considering these results, it is important to note that the tasks used in the two studies described above rely on different neural populations within the visual system. Although motion-sensitive neural populations exist in both V1 and area MT (13), the ability to detect coherent motion in random dot kinematograms is specifically dependent on MT neurons that have large receptive fields and are able to integrate global motion information (14, 15). Conversely, performance in a contrast discrimination task is based on the accurate responses of V1 neurons without the need for spatial integration (18). Indeed, MT neurons are not sensitive to contrast (19, 20) and MT lesions impair the perception of coherent motion but do not affect contrast discrimination thresholds (21).

Since both tasks rely on initial computations performed by motion/contrast-sensitive neurons in V1 and since EEG recordings cannot distinguish between the activity of V1 and MT neurons, it is possible that the variability quenching reported in both studies was generated by overlapping neural populations in V1. Nevertheless, we demonstrate that the relationship between neural variability quenching and perceptual performance appears consistently in different visual tasks that require different neural computations and are dependent on different visual system areas. Additional studies assessing this relationship using perceptual tasks in other sensory modalities are highly warranted for determining the generalizability of this phenomenon across sensory domains and perceptual tasks.

Neural Variability and Perception

The principles of signal detection theory suggest that detection of a stimulus depends on two key factors: the strength of the stimulus and the magnitude of the noise/variability masking the stimulus (12). One form of noise is spatial noise that can be added to a visual stimulus, thereby degrading the stimulus and making it more difficult to identify. Gradually increasing the amount of spatial noise enables behavioral estimation of the internal noise of a neural system by using the equivalent noise technique (40). Indeed, individuals with larger internal neural noise estimates exhibit poorer perceptual performance with higher thresholds (41, 42).

Another form of noise/variability is apparent in trial-by-trial variability, which reduces the reproducibility of neural responses across trials. Several studies have demonstrated that perception is more accurate when neural activity is less variable (i.e., more reproducible). For example, trials where a

threshold level visual stimulus was detected exhibit lower trial-by-trial variability than trials where the stimulus was not detected (43). Similarly, older individuals with larger trial-by-trial auditory response variability are less accurate at sound localization (44). Furthermore, trial-by-trial variability is actively reduced when allocating spatial attention to a visual stimulus (3, 45, 46, 47), potentially explaining the accuracy and speed benefits of attention.

Although trial-by-trial variability is clearly quenched after the presentation of a stimulus (1), individual subjects quench neural variability to different extents. Indeed, individual differences are consistently apparent when examining EEG recordings of the same subjects performed a year apart and when individuals perform different tasks with different stimuli (4). This suggests that the magnitude of variability quenching is an individual trait that is mostly determined by individual neurophysiology. The current and former (5) studies from our laboratory extend previous findings by consistently demonstrating that these individual differences are associated with the subjects' perceptual abilities such that individuals with larger variability quenching exhibit better perceptual thresholds.

Note that there was no group difference in variability quenching across the low and high dot-density conditions despite a group difference in perceptual thresholds (Fig. 3). This is in line with the suggestion that variability quenching is an individual neurophysiological trait that barely changes with task difficulty (Fig. 3B). Nevertheless, individuals who quenched neural variability to a larger degree exhibited lower perceptual thresholds particularly in situations where the strength of the stimulus was weak (i.e., lower dot density, Fig. 5) and the detection of coherent motion was more difficult as indicated by higher perceptual thresholds (Fig. 4) (48, 49). Hence, we suggest that the behavioral significance of individual differences in variability quenching is particularly evident in the detection of weak stimuli.

Absolute Neural Variability and Variability Quenching

Individual subjects differ in the absolute magnitudes of trial-by-trial variability that they exhibit as well as in the magnitude of variability quenching following stimulus presentation. Some studies have suggested that larger absolute variability is apparent in younger subjects and those with better cognitive abilities (50, 51). However, in our previous study, we reported that individual magnitudes of absolute variability were not correlated with contrast discrimination thresholds in healthy adults. Instead, only individual magnitudes of variability quenching were significantly correlated with discrimination thresholds (5). Here, we demonstrate similar findings with respect to coherent-motion thresholds. Individual magnitudes of variability quenching were correlated with coherent-motion thresholds and not measures of absolute variability in pre- or poststimulus periods. Hence, our results highlight the importance of relative rather than absolute variability measures for explaining, at least in part, individual differences in perceptual abilities.

Measurement Noise

Trial-by-trial neural variability may be affected by measurement noise that may differ across subjects. One potential

source of measurement noise in EEG recordings is the quality of the EEG recording. When using active electrode systems, the quality of individual recordings can be estimated by measuring very low-frequency changes that are apparent in electrode offset differences across trials (see METHODS). Individual differences in electrode offset variability across trials, however, were not correlated with variability quenching magnitudes. This indicated that our results were not driven by potential differences in EEG recording quality across subjects. Another potential source of variability is differences in the amount of eye movements across subjects (37). Therefore, we computed eye-gaze variability of individual subjects, which quantified the amount of eye movements (i.e., inverse of fixation stability). This measure was also not correlated with variability quenching magnitudes, demonstrating that our results were not driven by potential between-subject differences in eye movements.

Conclusions

Individual differences in the magnitudes of neural variability quenching are associated with individual perceptual abilities in the visual domain as demonstrated in both contrast discrimination and motion coherence tasks. Additional studies demonstrate that larger variability is apparent in the elderly, where perceptual abilities are poorer (44), and that attention reduces variability across trials while improving perceptual performance (3, 45). In line with signal detection theory principles, these findings add additional support to the hypothesis that cortical sensory networks increase cortical reproducibility to enhance detection and discrimination of sensory stimuli.

GRANTS

This work was supported by the Israeli Science Foundation (Grant 961/14 to I. Dinstein).

DISCLOSURES

No conflicts of interest, financial or otherwise, are declared by the authors.

AUTHOR CONTRIBUTIONS

E.D. and I.D. conceived and designed research; E.D. performed experiments; E.D. analyzed data; E.D. and I.D. interpreted results of experiments; E.D. prepared figures; E.D. drafted manuscript; E.D. and I.D. edited and revised manuscript; E.D. and I.D. approved final version of manuscript.

REFERENCES

1. Churchland MM, Yu BM, Cunningham JP, Sugrue LP, Cohen MR, Corrado GS, Newsome WT, Clark AM, Hosseini P, Scott BB, Bradley DC, Smith MA, Kohn A, Movshon JA, Armstrong KM, Moore T, Chang SW, Snyder LH, Lisberger SG, Priebe NJ, Finn IM, Ferster D, Ryu SI, Santhanam G, Sahani M, Shenoy KV. Stimulus onset quenches neural variability: a widespread cortical phenomenon. *Nat Neurosci* 13: 369–378, 2010. doi:10.1038/nn.2501.
2. Churchland MM, Yu BM, Ryu SI, Santhanam G, Shenoy KV. Neural variability in premotor cortex provides a signature of motor preparation. *J Neurosci* 26: 3697–3712, 2006. doi:10.1523/JNEUROSCI.3762-05.2006.

3. **Arazi A, Yeshurun Y, Dinstein I.** Neural variability is quenched by attention. *J Neurosci* 39: 5975–5985, 2019. doi:10.1523/jneurosci.0355-19.2019.
4. **Arazi A, Gonen-Yaacovi G, Dinstein I.** The magnitude of trial-by-trial neural variability is reproducible over time and across tasks in humans. *eNeuro* 4: ENEURO.0292-17.2017, 2017. doi:10.1523/ENEURO.0292-17.2017.
5. **Arazi A, Censor N, Dinstein I.** Neural variability quenching predicts individual perceptual abilities. *J Neurosci* 37: 97–109, 2017. doi:10.1523/JNEUROSCI.1671-16.2016.
6. **Brodav-Dvir R, Grossman S, Furman-Haran E, Malach R.** Quenching of spontaneous fluctuations by attention in human visual cortex. *Neuroimage* 171: 84–98, 2018. doi:10.1016/j.neuroimage.2017.12.089.
7. **Gao R.** Interpreting the electrophysiological power spectrum. *J Neurophysiol* 115: 628–630, 2016. doi:10.1152/jn.00722.2015.
8. **He BJ.** Spontaneous and task-evoked brain activity negatively interact. *J Neurosci* 33: 4672–4682, 2013. doi:10.1523/JNEUROSCI.2922-12.2013.
9. **He BJ, Zempel JM.** Average is optimal: an inverted-U relationship between trial-to-trial brain activity and behavioral performance. *PLoS Comput Biol* 9: e1003348, 2013. doi:10.1371/journal.pcbi.1003348.
10. **Schurger A, Sarigiannidis I, Naccache L, Sitt JD, Dehaene S.** Cortical activity is more stable when sensory stimuli are consciously perceived. *Proc Natl Acad Sci USA* 112: E2083–E2092, 2015. doi:10.1073/pnas.1418730112.
11. **Daniel E, Meindertsma T, Arazi A, Donner TH, Dinstein I.** The relationship between trial-by-trial variability and oscillations of cortical population activity. *Sci Rep* 9: 16901, 2019. doi:10.1038/s41598-019-53270-7.
12. **Green DM, Swets JA.** *Signal Detection Theory and Psychophysics*. New York: Wiley, 1966. doi:10.1901/jeab.1969.12-475.
13. **Born RT, Bradley DC.** Structure and visual function of area MT. *Annu Rev Neurosci* 28: 157–189, 2005. doi:10.1146/annurev.neuro.26.041002.131052.
14. **Kumano H, Uka T.** Responses to random dot motion reveal prevalence of pattern-motion selectivity in area MT. *J Neurosci* 33: 15161–15170, 2013. doi:10.1523/JNEUROSCI.4279-12.2013.
15. **Van Wezel RJA, Britten KH.** Motion adaptation in area MT. *J Neurophysiol* 88: 3469–3476, 2002. doi:10.1152/jn.00276.2002.
16. **Salzman CD, Britten KH, Newsome WT.** Cortical microstimulation influences perceptual judgements of motion direction. *Nature* 346: 174–177, 1990 [Erratum in *Nature* 346: 589, 1990]. doi:10.1038/346174a0.
17. **Rust NC, Mante V, Simoncelli EP, Movshon JA.** How MT cells analyze the motion of visual patterns. *Nat Neurosci* 9: 1421–1431, 2006. doi:10.1038/nn1786.
18. **Albrecht DG, Hamilton DB.** Striate cortex of monkey and cat: contrast response function. *J Neurophysiol* 48: 217–237, 1982. doi:10.1152/jn.1982.48.1.217.
19. **Tootell RB, Hadjikhani NK, Vanduffel W, Liu AK, Mendola JD, Sereno MI, Dale AM.** Functional analysis of primary visual cortex (V1) in humans. *Proc Natl Acad Sci USA* 95: 811–817, 1998. doi:10.1073/pnas.95.3.811.
20. **Tootell RB, Reppas JB, Kwong KK, Malach R, Born RT, Brady TJ, Rosen BR, Belliveau JW.** Functional analysis of human MT and related visual cortical areas using magnetic resonance imaging. *J Neurosci* 15: 3215–3230, 1995. doi:10.1523/JNEUROSCI.15-04-03215.1995.
21. **Newsome WT, Pare EB.** A selective impairment of motion perception following lesions of the middle temporal visual area (MT). *J Neurosci* 8: 2201–2211, 1988. doi:10.1523/jneurosci.08-06-02201.1988.
22. **Cornelissen P, Richardson A, Mason A, Fowler S, Stein J.** Contrast sensitivity and coherent motion detection measured at photopic luminance levels in dyslexics and controls. *Vision Res* 35: 1483–1494, 1995. doi:10.1016/0042-6989(95)98728-R.
23. **Milne E, Swettenham J, Hansen PC, Campbell R, Jefferies H, Plaisted K.** High motion coherence thresholds in children with autism. *J Child Psychol Psychiatry* 43: 255–263, 2002. doi:10.1111/1469-7610.00018.
24. **Talcott JB, Hansen PC, Willis-Owen C, McKinnell IW, Richardson AJ, Stein JF.** Visual magnocellular impairment in adult developmental dyslexics. *J Neuroophthalmol* 20: 187–201, 1998. doi:10.1076/noph.20.4.187.3931.
25. **Downing C, Movshon J.** Spatial and temporal summation in the detection of motion in stochastic random dot displays. *Invest Ophthalmol Vis Sci* 30: 72, 1989.
26. **Brainard DH.** The psychophysics toolbox. *Spat Vis* 10: 433–436, 1997. doi:10.1163/156856897X00357.
27. **Kleiner M, Brainard DH, Pelli DG, Broussard C, Wolf T, Niehorster D.** What's new in Psychtoolbox-3? *Perception* 36: 1–16, 2007. doi:10.1068/v070821.
28. **Pelli DG.** The VideoToolbox software for visual psychophysics: transforming numbers into movies. *Spat Vis* 10: 437–442, 1997. doi:10.1163/156856897X00366.
29. **Kingdom FAA, Prins N.** *Psychophysics: A Practical Introduction*. London, UK: Elsevier Academic Press, 2016.
30. **Kontsevich LL, Tyler CW.** Bayesian adaptive estimation of psychometric slope and threshold. *Vision Res* 39: 2729–2737, 1999. doi:10.1016/S0042-6989(98)00285-5.
31. **Hall JL.** Maximum-likelihood sequential procedure for estimation of psychometric functions. *J Acoust Soc Am* 44: 370, 1968. doi:10.1121/1.1970490.
32. **Watson AB, Pelli DG.** Quest: a Bayesian adaptive psychometric method. *Percept Psychophys* 33: 113–120, 1983. doi:10.3758/bf03202828.
33. **Prins N, Kingdom FAA.** Applying the model-comparison approach to test specific research hypotheses in psychophysical research using the Palamedes toolbox. *Front Psychol* 9: 1250, 2018. doi:10.3389/fpsyg.2018.01250.
34. **Delorme A, Makeig S.** EEGLAB: an open source toolbox for analysis of single-trial EEG dynamics including independent component analysis. *J Neurosci Methods* 134: 9–21, 2004. doi:10.1016/j.jneumeth.2003.10.009.
35. **Dimigen O, Sommer W, Hohlfeld A, Jacobs AM, Kliegl R.** Coregistration of eye movements and EEG in natural reading: analyses and review. *J Exp Psychol Gen* 140: 552–572, 2011. doi:10.1037/a0023885.
36. **Kappenman ES, Luck SJ.** The effects of electrode impedance on data quality and statistical significance in ERP recordings. *Psychophysiology* 47: 888–904, 2010. doi:10.1111/j.1469-8986.2010.01009.x.
37. **Yuval-Greenberg S, Tomer O, Keren AS, Nelken I, Deouell LY.** Transient induced gamma-band response in EEG as a manifestation of miniature saccades. *Neuron* 58: 429–441, 2008. doi:10.1016/j.neuron.2008.03.027.
38. **JASP Team.** JASP (Version 0.12.2), 2020. <https://jasp-stats.org/download/>
39. **Dienes Z.** Using Bayes to get the most out of non-significant results. *Front Psychol* 5: 781, 2014. doi:10.3389/fpsyg.2014.00781.
40. **Allard R, Faubert J, Pelli DG.** Editorial: using noise to characterize vision. *Front Psychol* 6: 1707, 2015. doi:10.3389/fpsyg.2015.01707.
41. **Legge GE, Kersten D, Burgess AE.** Contrast discrimination in noise. *J Opt Soc Am A* 4: 391–404, 1987. doi:10.1364/josaa.4.000391.
42. **Pardhan S.** Contrast sensitivity loss with aging: sampling efficiency and equivalent noise at different spatial frequencies. *J Opt Soc Am A Opt Image Sci Vis* 21: 169–175, 2004. doi:10.1364/josaa.21.000169.
43. **Schurger A, Pereira F, Treisman A, Cohen JD.** Reproducibility distinguishes conscious from nonconscious neural representations. *Science* 327: 97–99, 2010. doi:10.1126/science.1180029.
44. **Anderson S, Parbery-Clark A, White-Schwach T, Kraus N.** Aging affects neural precision of speech encoding. *J Neurosci* 32: 14156–14164, 2012. doi:10.1523/JNEUROSCI.2176-12.2012.
45. **Cohen MR, Maunsell JHR.** Attention improves performance primarily by reducing interneuronal correlations. *Nat Neurosci* 12: 1594–1600, 2009. doi:10.1038/nn.2439.
46. **Mitchell JF, Sundberg KA, Reynolds JH.** Spatial attention decorrelates intrinsic activity fluctuations in macaque area V4. *Neuron* 63: 879–888, 2009. doi:10.1016/j.neuron.2009.09.013.
47. **Mitchell JF, Sundberg KA, Reynolds JH.** Differential attention-dependent response modulation across cell classes in macaque visual area V4. *Neuron* 55: 131–141, 2007. doi:10.1016/j.neuron.2007.06.018.

48. **Chen Y, Nakayama K, Levy D, Matthyse S, Holzman P.** Processing of global, but not local, motion direction is deficient in schizophrenia. *Schizophr Res* 61: 215–227, 2003. doi:10.1016/S0920-9964(02)00222-0.
49. **Watamaniuk SNJ, Grzywacz NM, Yuille AL.** Dependence of speed and direction perception on cinematogram dot density. *Vision Res* 33: 849–859, 1993. doi:10.1016/0042-6989(93)90204-A.
50. **Garrett DD, Kovacevic N, McIntosh AR, Grady CL.** The importance of being variable. *J Neurosci* 31: 4496–4503, 2011. doi:10.1523/JNEUROSCI.5641-10.2011.
51. **Grady CL, Garrett DD.** Understanding variability in the BOLD signal and why it matters for aging. *Brain Imaging Behav* 8: 274–283, 2014. doi:10.1007/s11682-013-9253-0.